Conf-9011279--1

NANOPHASE MATERIALS ASSEMBLED FROM CLUSTERS*

Richard W. Siegel
Materials Science Division
Argonne National Laboratory
Argonne, Illinois 60439 USA

ANL/CP--75656

DE92 010508

February 1992

DISCLAIMER

Invited paper to be published in the Proceedings of the International Symposium on Materials for Advanced Technology Systems, 1990 Annual Technical Meeting of the Indian Institute of Metals, Tiruchirapalli, India, November 14-17, 1990.

*Work supported by the U. S. Department of Energy, BES-Materials Sciences, under Contract W-31-109-Eng-38.

Invited paper to be published in the Proceedings of the International Symposium on Materials for Advanced Technology Systems, 1990 Annual Technical Meeting of the Indian Institute of Metals, Tiruchirapalli, India, November 14-17, 1990.

NANOPHASE MATERIALS ASSEMBLED FROM CLUSTERS

Richard W. Siegel
Materials Science Division, Argonne National Laboratory, Argonne, Illinois 60439 USA

ABSTRACT

The preparation of metal and ceramic atom clusters by means of the gas-condensation method, followed by their *in situ* collection and consolidation under high-vacuum conditions, has recently led to the synthesis of a new class of ultrafine-grained materials. These nanophase materials, with typical average grain sizes of 5 to 50 nm and, hence, a large fraction of their atoms in interfaces, exhibit properties that are often considerably improved relative to those of conventional materials. Furthermore, their synthesis and processing characteristics should enable the design of new materials with unique properties. Some examples are ductile ceramics that can be formed and sintered to full density at low temperatures without the need for binding or sintering aids, and metals with dramatically increased strength. The synthesis of these materials is briefly described along with what is presently known of their structure and properties. Their future impact on materials science and technology is also considered.

1. INTRODUCTION

In the past few years, considerable interest has focussed on materials with ultrafine microstructures in the nanometer size range owing to their novel properties and the increasing potential to engineer these materials from atomic or molecular precursors [1]. Among the wide variety of synthesis and processing methods available for producing such nanophase materials, atom cluster assembly [2, 3] appears to have unique advantages. The synthesis of materials with ultrafine microstructures by the *in situ* consolidation of gas-condensed particles or atom clusters was first apparently suggested by

Gleiter [4] based upon a considerable body of earlier research into the production of ultrafine particles by means of the gas-condensation method [5-8] and the extensive history of powder metallurgy and ceramics. The previous research on the gas-condensation method, and on the atom clusters produced using this method, defined the parameters (primarily the type of gas used, its pressure, and the precursor evaporation rate) that control the sizes of the clusters formed in the conventional gas-condensation method that is presently being used to synthesize nanophase materials. Based upon the research completed to date [3, 9], it appears certain that this method combined with cluster assembly should in the future enable the design of materials heretofore unavailable with either improved or unique properties. As such, the assembly of atom clusters to form nanophase materials will likely have a significant impact on materials science and engineering in the coming years.

The research on cluster-assembled nanophase materials that has been completed to date has relied on the conventional gas-condensation method, which utilizes convective gas flow. Using this method, the average cluster diameters attainable have ranged between about 5 and 50 nm, yielding upon consolidation nanophase materials with such grain sizes. Nevertheless, other applications of the gas-condensation method that utilize forced gas flow have been widely used by cluster chemists and physicists to produce low yields of even smaller monosized atomic clusters [2]. Cluster sources based on similar physical principles will likely become available in the future for the generation of larger yields of clusters that will be useful for assembly into nanophase materials. While nanophase materials can in principle be metals, ceramics, semiconductors, or composites thereof, and they can contain phases on a nanometer scale with crystalline, quasicrystalline, or amorphous structure, most of the research carried out to date has concentrated on single-phase metals and ceramics. This short review will consider some of the highlights of the research thus far completed on cluster-assembled materials.

2. SYNTHESIS AND PROCESSING

The synthesis of nanophase materials from gas-condensed atom clusters has been described in several papers [3, 9-14]. An apparatus that has been used in our laboratory during the past several

years for the synthesis of gas-consensed cluster-consolidated nanophase materials is shown schematically in Fig 1. It is comprised of an ultrahigh-vacuum (UHV) system fitted with two resistively-heated evaporation sources, a cluster collection device (liquid-nitrogen filled cold finger) and scraper assembly, and *in situ* compaction devices for consolidating the powders produced and collected in the chamber.

The UHV system is first evacuated by means of a turbomolecular pump to below 10^{-5} Pa and then back-filled with a controlled high-purity gas atmosphere at pressures of about a few hundred Pa. For producing metal powders this is usually an inert gas, such as He, but it can alternatively be a reactive gas or gas mixture if, for example, clusters of a ceramic compound are desired. During evaporation of the precursor material (or materials) from which the nanophase material will be synthesized, atoms lose energy via collisions with the gas atoms and condense in the highly supersaturated region close to the source. Since the gas is moving via the natural convective flow driven by gravity and the temperature difference between source and collecter, the gas-entrained clusters are transported in the gas to the liquid-nitrogen filled cold finger, where they are collected via thermophoresis. The condensing gas type and pressure and the material evaporation rate, which are all easily controlled, determine the resulting particle-size distributions in such an apparatus [6].

In the apparatus shown in Fig. 1, and in other natural convection systems of this general type, Joule-heated evaporation sources are most often used in producing clusters for nanophase material. However, a wide range of other evaporation sources [8] can be applied to this process, including sputtering [15-19], plasma [20], electron beam [21-24], or laser ablation [25] methods, for example, that will give a much wider range of flexibility and eventual control in the synthesis of nanophase materials. Furthermore, the gas-entrained transport of the condensed atom clusters via natural gas convection can be improved upon by using instead the motion of a forced gas. Forced gas flow is already used in the more sophisticated cluster synthesis methods [2], and it will, among other advantages, greatly facilitate the synthesis of nanophase materials with even smaller grain sizes and also the collection of larger amounts of material than are normally produced in natural convection systems.

The clusters collected on the surface of the cold finger form very open, fractal or tree-like structures [26]. These are easily removed from this collection surface by means of a Teflon scraper and collected via a funnel into piston-and-anvil devices (Fig. 1) capable of compaction pressures up to about 1-2 GPa, in which the consolidated nanophase compacts are formed at room temperature. The samples are typically about 9 mm in diameter and 0.1 to 0.5 mm thick, depending upon the amount of material made (usually a few hundred milligrams) and the experiments to be performed. The scraping and consolidation are performed under UHV conditions after removal of the inert or reactive gases from the chamber, in order to maximize the cleanliness of the particle surfaces and the interfaces that are subsequently formed, while minimizing any possibility of trapping remnants of these gases in the nanophase sample. It should be noted in this regard that the total surface area of the nanophase powders produced in a given run is so great that, for a residual gas pressure of less than 10^{-5} Pa in a volume the size of the UHV chamber used, little gas contamination of the cluster surfaces would be expected.

There are a number of advantages associated with the synthesis of nanophase materials from atom clusters. Some of these stem from the nanometer scale of the structures assembled and others arise from the inherent flexibility of dealing with clusters as the building blocks of these materials. Some of these advantages are as follows [3]:

(1) The ultrafine sizes of the atom clusters and their surface cleanliness allow conventional restrictions of phase equilibria and kinetics to be overcome during material synthesis and processing, by the combination of short diffusion distances, high driving forces, and uncontaminated surfaces and interfaces.

(2) The large fraction of atoms residing in the grain boundaries and interfaces of these materials allow for interface atomic arrangements to constitute significant volume fractions of material, and thus novel materials properties may result.

(3) The reduced size scale and large surface-to-volume ratios of the individual nanophase grains can be predetermined and can alter and enhance a variety of physical and chemical properties.

(4) A wide range of materials can be produced in this manner including, in addition to metals and alloys, intermetallic compounds, ceramics, and semiconductors. It is also apparent that they can be formed to contain crystalline, quasicrystalline, or amorphous structures.

(5) The possibilities for reacting, coating, and mixing in situ various types, sizes, and morphologies of clusters create a significant potential for the synthesis of a variety of new multicomponent composites with nanometer-sized microstructures and engineered properties.

3. STRUCTURE

The structures of cluster-assembled nanophase materials, both metals and oxides, have been investigated by a number of direct and indirect methods including transmission electron microscopy [26-29], x-ray [30-33] and neutron [34-36] scattering, and Mössbauer [37, 38], Raman [39-41], and positron annihilation [26, 42, 43] spectroscopy. It has been found that the grains in nanophase compacts are typically rather equiaxed, as are the clusters from which they were assembled, and retain the narrow log-normal size distributions representative of the clusters formed in the gas-condensation method [6]. Their grain sizes, moreover, remain rather deeply metastable to elevated temperatures [44].

Figure 2 shows a typical area of a nanophase palladium sample with about 5-6 nm grain size as seen by high resolution transmission electron microscopy [28]. A typical log-normal grain size distribution for a nanophase sample, in this case TiO_2 with the rutile structure [26] is shown in the inset of Fig. 3. This type of size distribution is a natural consequence of the homogeneous nucleation of clusters combined with the cluster-cluster coalescence that occurs in the gas-condensation process under natural convection conditions [6]. The 12 nm initial average grain diameter for this distribution changes little with annealing to elevated temperatures until about 40-50% of the sample's absolute melting temperature is reached, as also shown in Fig. 3. This behavior appears to be rather typical for nanophase oxides [14], and for nanophase metals as well, as shown in Fig. 4 [44].

Since a large fraction of their atoms reside in the grain boundaries of nanophase materials, the interface structures can play a significant role, along with the reduced size of the grains themselves, in determining the properties of these materials. As such, a number of experimental investigations have focussed on the grain boundary structures in nanophase materials. A variety of investigations

on nanocrystalline metals by Gleiter and coworkers [46], have been interpreted in terms of grain boundary atomic structures that may be random, rather than possessing either the short-range or long-range order normally found in the grain boundaries of coarser-grained polycrystalline materials. However, recent investigations of nanophase TiO_2 by Raman spectroscopy [39, 40] and of nanophase palladium by high resolution electron microscopy (HREM) [27, 28] indicate that the grain boundary structures in these materials are quite normal and rather like those of high angle grain boundaries in conventional polycrystals [47].

According to these investigations, the nanophase grain boundaries appear to contain short-range ordered structural units representative of the bulk material and distortions that are localized to about $\pm$ 0.2 nm on either side of the grain boundary plane. The latter result is also consistent with the observed small angle neutron scattering from nanophase samples [34, 36]. These conclusions regarding conventional grain boundary structures are also consistent with the expectations from condensed matter theory [48, 49] and the known healing distances in these materials. Similarly, recent HREM investigations of the grain boundaries of nanophase materials produced by mechanical attrition also support these conclusions [50, 51]. An extensive review of the issues regarding grain boundary structures in nanophase materials will appear elsewhere [52].

Positron annihilation spectroscopy (PAS) has been a useful tool in the study of the inherently ultrafine-scale porosity in nanophase compacts [26, 42, 43], which can be probed to advantage by PAS as a function of sintering temperature to observe densification. An example of PAS lifetime results [26] used to follow the sintering behavior of nanophase TiO_2 is shown in Fig. 5. The intensity I_2 of the lifetime (τ_2) signal corresponding to positron annihilation from void-trapped states in the nanophase sample is seen to decrease rapidly during sintering above 500°C as a result of the densification of this ultrafine-grained ceramic, even though rapid grain growth does not set in until above 800°C. Furthermore, the variation of τ_2 with sintering indicates that there is a redistribution of void sizes accompanying this densification that can also be followed by PAS. Similar behavior is also observed in the results for the coarser-grained samples shown in Fig. 5. However, as expected, the densification proceeds more slowly in these latter samples and the pore sizes are larger according to the larger values of τ_2.

4. PROPERTIES

The properties of nanophase materials are often considerably altered and improved in comparison with those of conventional structures owing to various combinations of their reduced grain sizes, significant volume fraction of uncontaminated interfaces, and clean and reactive cluster surfaces. For example, nanophase TiO_2 (rutile) exhibits considerable improvements in both the sinterability and resulting mechanical properties of this material relative to conventionally synthesized rutile [26].

Results of microhardness measurements as a function of sintering temperature for nanophase TiO_2 with an initial average grain size of 12 nm are compared in Fig. 6 with similar measurements on two coarser-grained samples produced from commercial TiO_2 powders ball-milled to 1.3 μm average diameter [26]. The nanophase TiO_2 is seen to sinter at 400 to 600°C lower temperatures than the coarser-grained material, and without the need for the compacting and sintering aid polyvinyl alcohol (pva); without pva the commercial TiO_2 did not effectively sinter. Also, the resulting fracture characteristics [53-55] developed for the nanophase TiO_2 appear to be better than those for conventional rutile.

It may not be terribly surprising that nanophase ceramics, with their ultrafine grain sizes, clean cluster surfaces, and high grain boundary purity, will sinter at much lower temperatures than conventional coarser-grained ceramics. However, it is unique that they can also retain their fine grain sizes after sintering to full density and exhibit superior mechanical properties as well. The ability to further decrease the sintering temperature of this material by pressure assisted sintering or by means of appropriate dopants while further suppressing grain growth [54, 56], as shown in Fig. 7, gives further support to the conclusion that stable nanophase ceramics with ultrafine grain sizes and theoretical densities can indeed be achieved and utilized.

In addition to their enhanced sinterability, the formability of nanophase ceramics is a further distinct advantage to these ultrafine-grained materials. This formability is clearly evident in the sample compaction process [26] and it has been demonstrated through deformation [57-59] as well. The

degree to which nanophase ceramics are truly ductile is only beginning to be understood. Nanoindenter measurements on nanophase TiO_2 [60] and ZnO [61], shown in Fig. 8, have recently demonstrated that a dramatic increase of strain rate sensitivity occurs with decreasing grain size in the nanophase regime, which appears to be generic to nanophase ceramics. The strain rate sensitivity values at the smallest grain sizes yet investigated (12 nm for TiO_2, 6 nm for ZnO) indicate ductile behavior of these ceramics, as well as a significant potential for increased ductility at even smaller grain sizes and elevated temperatures (below those at which significant grain growth will occur). The ductility of these nanophase ceramics appears to result from grain boundary sliding in these materials, which becomes more prevalent as their grain sizes decrease and the diffusion distances necessary for intergrain healing become shorter.

In contrast to nanophase oxides, where the microhardness of as-compacted samples is reduced relative to their fully dense counterparts owing to significant porosity in addition to their ultrafine grain sizes, the case for nanophase metals is quite different. Figure 9 shows recent microhardness results for several nanophase copper samples compared with those for a coarser-grained sample [62]. In the as-compacted state, the nanophase samples are seen to increase in strength with decreasing grain size, with the 6-nm grain size nanophase sample exhibiting a five-fold increase in hardness over the coarser-grained (50 μm) sample. Similar increases in hardness [63] and yield stess [64], the latter shown in Fig. 10, were also observed in nanophase palladium, indicating that this grain-size dependent strengthening is apparently generic to nanophase metals. This is further supported by measurements on mechanically reduced nanostructured metals [65]. While this effect seems superficially analogous to the grain-boundary barrier, Hall-Petch strengthening observed in coarser-grained metals, it is in this case most likely a result of an increased difficulty in forming dislocations in the confined volumes of the nanophase grains, in which the critical stress to activate Frank-Read dislocation sources has greatly increased.

Atomic diffusion in nanophase materials, which may have a significant bearing on their mechanical properties such as creep at elevated temperatures, has also been found to be quite interesting. Measurements of self-diffusion and impurity-diffusion [66-68] in as-consolidated nanocrystalline metals and ceramics indicate that atomic transport is orders of magnitude faster in these materials

than in coarser-grained polycrystalline samples. However, this very rapid diffusion appears to be intrinsically coupled with the porous nature of the interfaces in these materials, and can be suppressed back to conventional values by sintering to full densities [54]. Nonetheless, there seem to exist considerable possibilities for efficiently doping nanophase materials via the rapid diffusion available along their ubiquitous grain-boundary networks to synthesize materials with tailored optical, electrical, or mechanical properties.

5. THE FUTURE

It is clear that in such a broad field as this, we are just beginning to scratch the surface of the tremendous opportunities for synthesizing nanophase materials via the assembly of atom clusters. The prognosis for the field has been recently considered [69] and will for the most part be repeated here. Based upon the limited knowledge that has already been accumulated, the future appears to hold great promise for nanophase materials. The cluster sizes accessed to date indicate that the high reactivities and short diffusion distances available in cluster-assembled materials can have profound effects upon the processing characteristics of these materials. These characteristics should be further enhanced as even smaller and more uniformly sized clusters become available in sufficiently large numbers to effect their assembly into usable and commercially viable materials.

The enhanced diffusivities along their grain boundary networks, with only few atomic jumps separating grain interiors from grain boundaries, should enable efficient impurity doping of these materials. Nanophase insulators and semiconductors, for example, could be easily doped with impurities at relatively low temperatures allowing efficient introduction of impurity levels into their band gaps and control over their electrical and optical properties. Moreover, the ability to produce via cluster assembly fully dense ultrafine-grained nanophase ceramics with controlled or flaw-free microstructures that are readily formable and exhibit ductility should have a significant technological impact in a wide variety of applications.

Research on cluster-assembled nanophase materials, although currently being carried out in only a few laboratories, appears now to be rapidly expanding [70, 71]. Much work still remains to be

done. Further research on the synthesis of a broader range of nanophase materials, encompassing metals, alloys, ceramics, semiconductors, and composites will have to be carried out in order to arrive at a fuller appreciation of just how broad an impact nanophase materials will have on materials technology. Investigations of their structure that will need to accompany such research will begin to elucidate the interplay between the effects of spatial confinement and large numbers of interfaces on the electrical, optical, magnetic, and mechanical properties of these new materials. A knowledge of the variation of such properties with the detailed structures and the synthesis and processing parameters of a variety of nanophase materials should eventually lead to an understanding of these new materials and consequently to the realization of their full technological potential in the future.

6. ACKNOWLEDGEMENTS

This work was supported by the U.S. Department of Energy, BES-Materials Sciences, under Contract W-31-109-Eng-38. The author wishes to thank his many collaborators at Argonne National Laboratory and elsewhere, without whose efforts and contributions much of the work referred in this paper would not have been accomplished.

7. REFERENCES

1. B. H. Kear, L. E. Cross, J. E. Keem, R. W. Siegel, F. Spaepen, K. C. Taylor, E. L. Thomas, and K.-N. Tu, **Research Opportunities for Materials with Ultrafine Microstructures** (National Academy, Washington, DC, 1989), Vol. NMAB-454.
2. R. P. Andres, R. S. Averback, W. L. Brown, L. E. Brus, W. A. Goddard, III, A. Kaldor, S. G. Louie, M. Moskovits, P. S. Peercy, S. J. Riley, R. W. Siegel, F. Spaepen, and Y. Wang, J. Mater. Res. **4**, 704 (1989).
3. R. W. Siegel, in **Materials Science and Technology**, Vol. 15, R. W. Cahn, ed. (VCH, Weinheim, 1991) p. 583.
4. H. Gleiter, in **Deformation of Polycrystals: Mechanisms and Microstructures**, N. Hansen et al., eds. (Risø National Laboratory, Roskilde, 1981) p. 15.

5. K. Kimoto, Y. Kamiya, M. Nonoyama, and R. Uyeda, Jpn. J. Appl. Phys. **2**, 702 (1963).

6. C. G. Granqvist and R. A. Buhrman, J. Appl. Phys. **47**, 2200 (1976).

7. A. R. Thölén, Acta Metall. **27**, 1765 (1979).

8. R. Uyeda, Prog. Mater. Sci. **35**, 1 (1991).

9. H. Gleiter, Prog. Mater. Sci. **33**, 223 (1989).

10. R. Birringer, U. Herr, and H. Gleiter, Suppl. Trans. Jpn. Inst. Met. **27**, 43 (1986).

11. R. W. Siegel and H. Hahn, in **Current Trends in the Physics of Materials**, M. Yussouff, ed. (World Scientific Publ. Co., Singapore, 1987) p. 403.

12. H. Hahn, J. A. Eastman, and R. W. Siegel, in Ceramic Transactions, **Ceramic Powder Science**, Vol. 1, Part B, G. L. Messing et al., eds. (American Ceramic Society, Westerville, 1988) p. 1115.

13. R. W. Siegel and J. A. Eastman, Mater. Res. Soc. Symp. Proc. **132**, 3 (1989).

14. J. A. Eastman, Y. X. Liao, A. Narayanasamy, and R. W. Siegel, Mater. Res. Soc. Symp. Proc. **155**, 255 (1989).

15. H. Oya, T. Ichihashi, and N. Wada, Jpn. J. Appl. Phys. **21**, 554 (1982).

16. S. Yatsuya, K. Yamauchi, T. Kamakura, A. Yanagada, H. Wakaiyama, and K. Mihama, Surface Sci. **156**, 1011 (1985).

17. S. Yatsuya, T. Kamakura, K. Yamauchi, and K. Mihama, Jpn. J. Appl. Phys., Part 2, **25**, L42 (1986).

18. H. Hahn and R. S. Averback, J. Appl. Phys. **67**, 1113 (1990).

19. G. M. Chow, R. L. Holtz, A. Pattnaik, A. S. Edelstein, T. E. Schlesinger, and R. C. Cammerata, Appl. Phys. Lett. **56**, 1853 (1990).

20. K. Baba, N. Shohata, and M. Yonezawa, Appl. Phys. Lett. **54**, 2309 (1989).

21. S. Iwama, E. Shichi, and T. Sahashi, Jpn. J. Appl. Phys. **12**, 1531 (1973).

22. S. Iwama, K. Hayakawa, and T. Arizumi, J. Cryst. Growth **56**, 265 (1982).

23. S. Iwama, K. Hayakawa, and T. Arizumi, J. Cryst. Growth **66**, 189 (1984).

24. S. Iwama and K. Hayakawa, Surface Sci. **156**, 85 (1985).

25. A. Matsunawa and S. Katayama, in **Laser Welding, Machining and Materials Processing**, Proc. ICALEO '85, C. Albright, ed. (IFS Publ. Ltd., 1985) p. 205.

26. R. W. Siegel, S. Ramasamy, H. Hahn, Z. Li, T. Lu, and R. Gronsky, J. Mater. Res. **3**, 1367 (1988).

27. G. J. Thomas, R. W. Siegel, and J. A. Eastman, Mater. Res. Soc. Symp. Proc. **153**, 13 (1989).

28. G. J. Thomas, R. W. Siegel, and J. A. Eastman, Scripta Metall. et Mater. **24**, 201 (1990).

29. W. Wunderlich, Y. Ishida, and R. Maurer, Scripta Metall. et Mater. **24**, 403 (1990).

30. X. Zhu, R. Birringer, U. Herr, and H. Gleiter, Phys. Rev. B **35**, 9085 (1987).

31. T. Haubold, R. Birringer, B. Lengeler, and H. Gleiter, J. Less-Common Metals **145**, 557 (1988).

32. T. Haubold, R. Birringer, B. Lengeler, and H. Gleiter, Phys. Lett. A **135**, 461 (1989).

33. M. R. Fitzsimmons, J. A. Eastman, M. Müller-Stach, G. Wallner, Phys. Rev. B **44**, 2452 (1991).

34. J. E. Epperson, R. W. Siegel, J. W. White, T. E. Klippert, A. Narayanasamy, J. A. Eastman, and F. Trouw, Mater. Res. Soc. Symp. Proc. **132**, 15 (1989).

35. E. Jorra, H. Franz, J. Peisl, G. Wallner, W. Petry, R. Birringer, H. Gleiter, and T. Haubold, Phil. Mag. B **60**, 159 (1989).

36. J. E. Epperson, R. W. Siegel, J. W. White, J. A.Eastman, Y. X. Liao, and A. Narayanasamy, Mater. Res. Soc. Symp. Proc. **166**, 87 (1990).

37. U. Herr, J. Jing, R. Birringer, U. Gonser, and H. Gleiter, Appl. Phys. Lett. **50**, 472 (1987).

38. J. Jiang, S. Ramasamy, R. Birringer, U. Gonser, and H. Gleiter, Solid State Commun. **80**, 525 (1991).

39. C. A. Melendres, A. Narayanasamy, V. A. Maroni, and R. W. Siegel, J. Mater. Res. **4**, 1246 (1989).

40. J. C. Parker and R. W. Siegel, J. Mater. Res. **5**, 1246 (1990).

41. J. C. Parker and R. W. Siegel, Appl. Phys. Lett. **57**, 943 (1990).

42. H. E. Schaefer, R. Würschum, M. Scheytt, R. Birringer, and H. Gleiter, Mater. Sci. Forum **15-18**, 955 (1987).

43. H. E. Schaefer, R. Würschum, R. Birringer, and H. Gleiter, Phys. Rev. B **38**, 9545 (1987).

44. R. W. Siegel, Mater. Res. Soc. Symp. Proc. **196**, 59 (1990).

45. E. Hort, Diploma Thesis, Universität des Saarlandes, Saarbrücken (1986).

46. R. Birringer and H. Gleiter, in **Encyclopedia of Materials Science and Engineering,** Suppl. Vol. 1, R. W. Cahn, ed. (Pergamon Press, Oxford, 1988) p. 339.
47. R. W. Siegel and G. J. Thomas, Mater. Res. Soc. Symp. Proc. **209**, 15 (1991).
48. S. R. Phillpot, D. Wolf, and S. Yip, MRS Bulletin **XV(10)**, 38 (1990).
49. D. Wolf and J. F. Lutsko, Phys. Rev. Lett. **60**, 1170 (1988).
50. S. K. Ganapathi and D. A. Rigney, Scripta Metall. et Mater. **24**, 1675 (1990).
51. M. L. Trudeau, A. Van Neste, and R. Schultz, Mater. Res. Soc. Symp. Proc. **206**, 487 (1991).
52. R. W. Siegel, in **Materials Interfaces: Atomic-Level Structure and Properties,** D. Wolf and S. Yip, eds. (Chapman and Hall, London, 1992) in press.
53. Z. Li, S. Ramasamy, H. Hahn, and R. W. Siegel, Mater. Lett. **6**, 195 (1988).
54. R. S. Averback, H. Hahn, H. J. Höfler, J. L. Logas, and T. C. Chen, Mater. Res. Soc. Symp. Proc. **153**, 3 (1989).
55. H. J. Höfler and R. S. Averback, Scripta Metall. et Mater. **24**, 2401 (1990).
56. H. Hahn, J. Logas, and R. S. Averback, J. Mater. Res. **5**, 609 (1990).
57. J. Karch, R. Birringer, and H. Gleiter, Nature **330**, 556 (1987).
58. R. Birringer and J. Karch, Ceramics International **16**, 291 (1990).
59. H. Hahn, J. Logas, H. J. Höfler, P. Kurath, and R. S. Averback, Mater. Res. Soc. Symp. Proc. **196**, 71 (1990).
60. M. J. Mayo, R. W. Siegel, A. Narayanasamy, and W. D. Nix, J. Mater. Res. **5**, 1073 (1990).
61. M. J. Mayo, R. W. Siegel, Y. X. Liao, and W. D. Nix, J. Mater. Res. **7**, in press (1992).
62. G. W. Nieman, J. R. Weertman, and R. W. Siegel, J. Mater. Res. **6**, 1012 (1991).
63. G. W. Nieman, J. R. Weertman, and R. W. Siegel, Scripta Metall. **23**, 2013 (1989).
64. G. W. Nieman, J. R. Weertman, and R. W. Siegel, Scripta Metall. et Mater. **24**, 145 (1990).
65. J. S. C. Jang and C. C. Koch, Scripta Metall. et Mater. **24**, 1599 (1990).
66. J. Horváth, R. Birringer, and H. Gleiter, Solid State Commun. **62**, 319 (1987).
67. J. Horváth, Defect and Diffusion Forum **66-69**, 207 (1989).
68. H. Hahn, H. Höfler, and R. S. Averback, Defect and Diffusion Forum **66-69**, 549 (1989).
69. R. W. Siegel, Ann. Rev. Mater. Sci. **21**, 559 (1991).

70. R. S. Averback, D. L. Nelson, and J. Bernholc, eds., **Clusters and Cluster-Assembled Materials**, Mater. Res. Soc. Symp. Proc. **206** (1991).

71. B. H. Kear, R. W. Siegel, and T. Tsakalakos, eds., Nanstructured Materials **1** (1992).

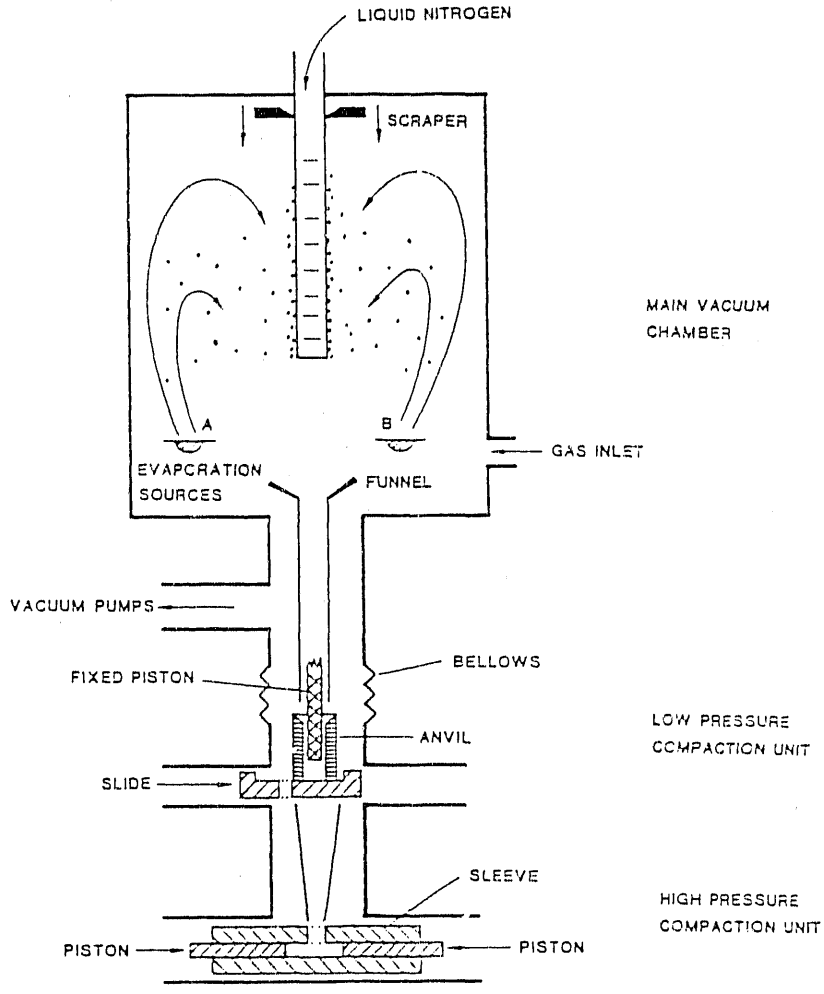

Figure 1. Schematic drawing of a gas-condensation chamber for the synthesis of nanophase materials. The material evaporated from sources A and/or B condenses in the gas and is transported via convection to the liquid-nitrogen filled cold finger. The powders are subsequently scraped from the cold finger, collected via the funnel, and consolidated first in the low-pressure compaction device and then in the high-pressure compaction device, all in vacuum. From [13].

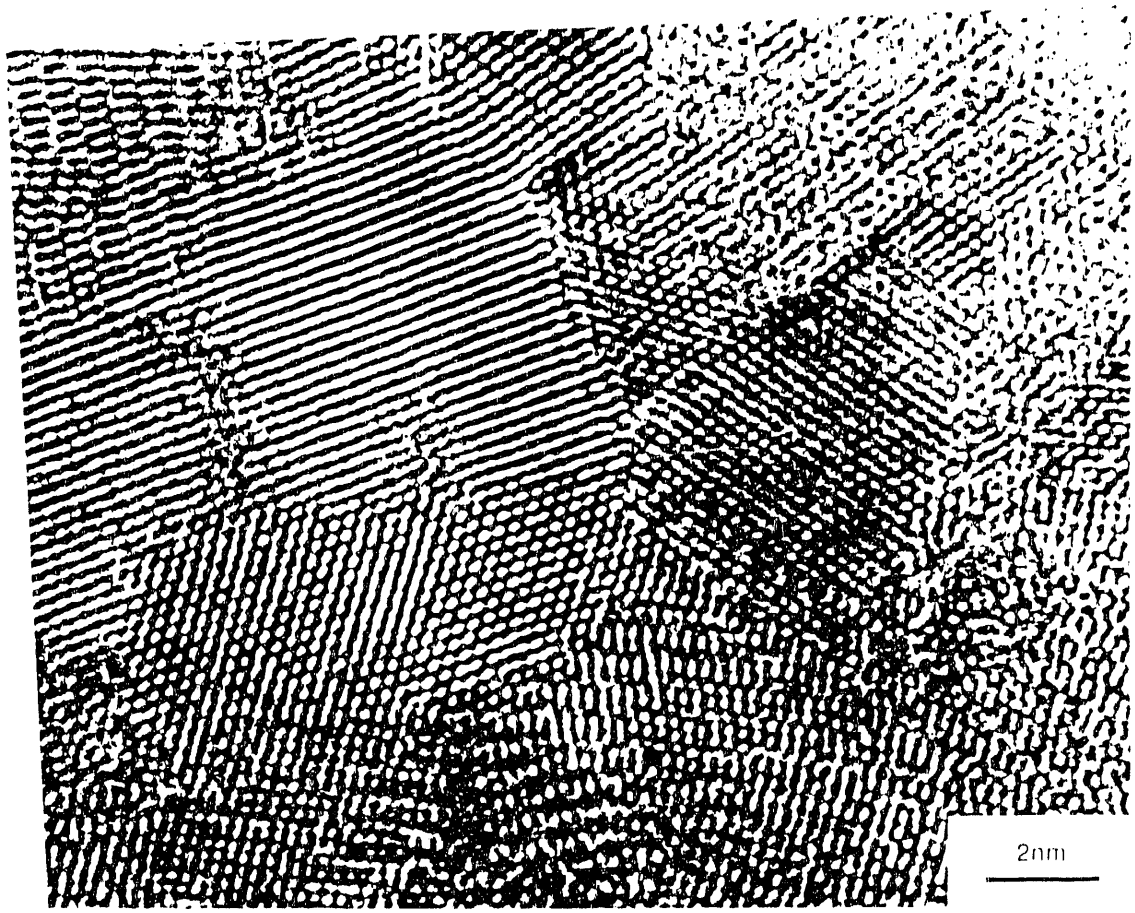

Figure 2. High resolution transmission electron micrograph of a typical area in nanophase palladium. From [28]. The magnification is indicated by the lattice fringe spacings, which are 0.195 nm ({002} planes) or 0.225 nm ({111} planes).

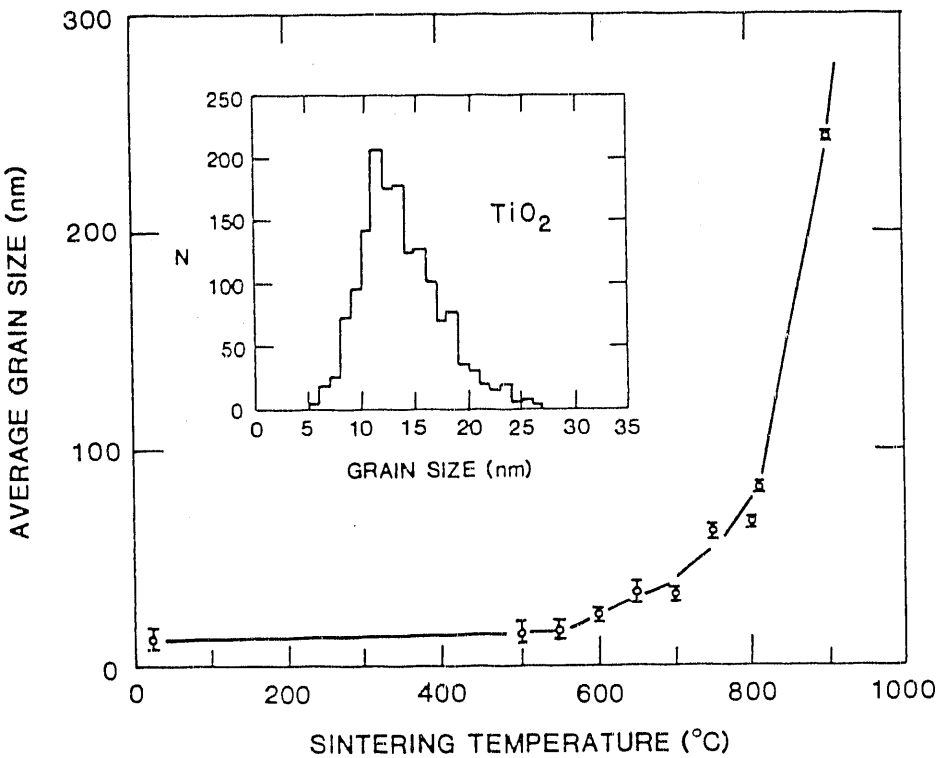

Figure 3. Grain size distribution for an as-consolidated nanophase TiO_2 (rutile) sample compacted to 1.4 GPa at room temperature, as determined by dark-field transmission electron microscopy (inset) and the variation of this average grain size with sintering temperature (0.5 h at each). After [26].

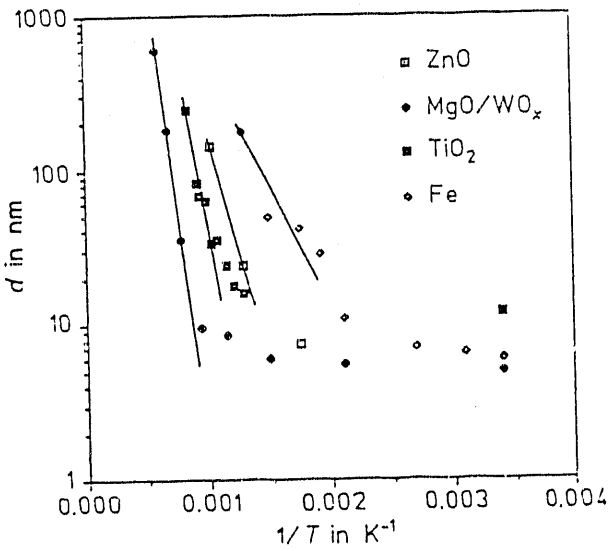

Figure 4. Arrhenius plot of the variation of average grain size, measured by dark-field transmission electron microscopy, with sintering temperature for nanophase Fe [45], TiO_2 [26], MgO/WO_X [14], and ZnO [14]. The oxide samples were annealed for one-half hour in air at each temperature; the iron for 10 hours in vacuum. From [44].

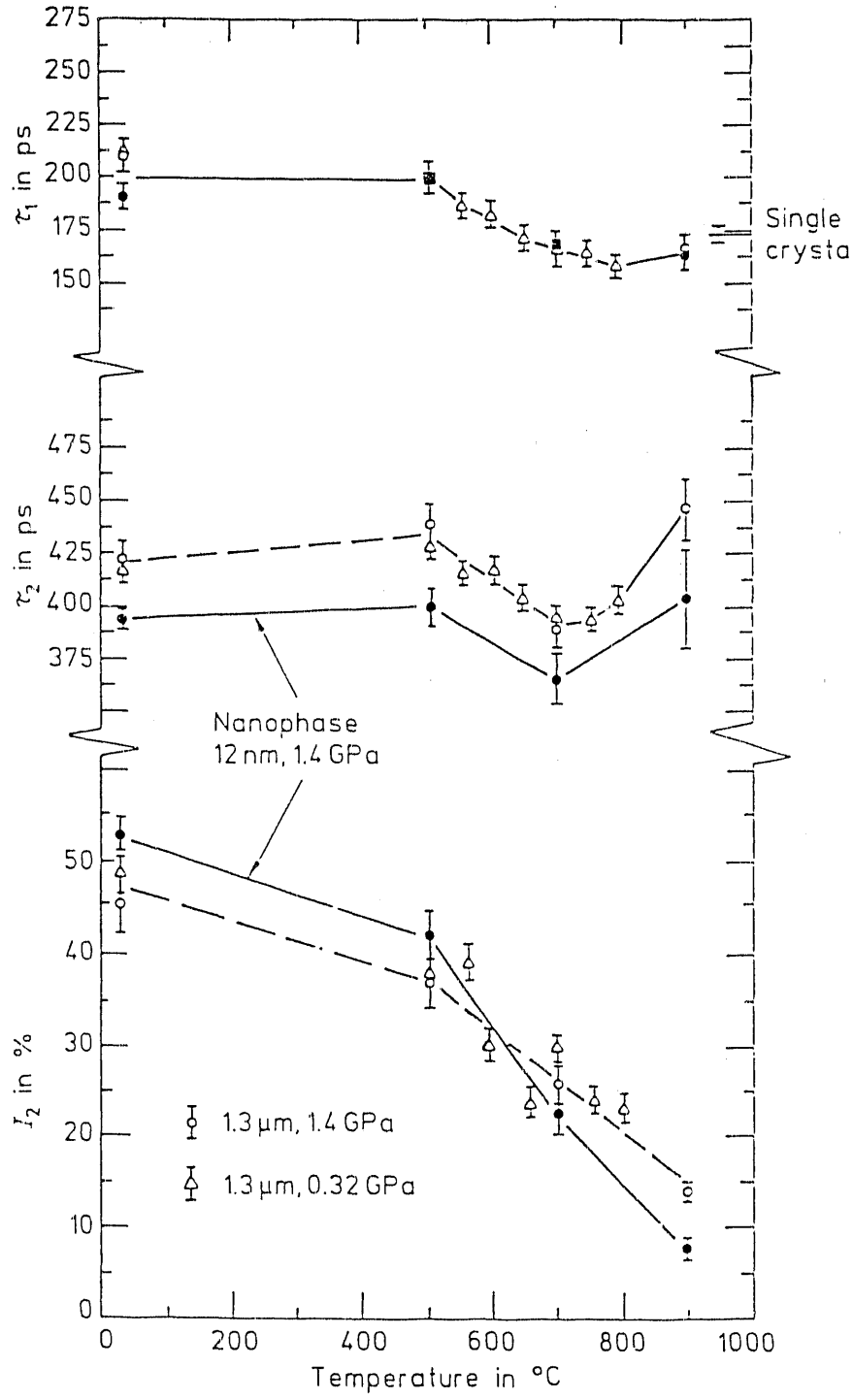

Figure 5. Results of two-component (τ_1, τ_2) lifetime fits to positron annihilation data from three TiO_2 samples as a function of sintering temperature. A 12 nm grain size nanophase sample (filled circles) compacted at 1.4 GPa is compared to 1.3 µm grain size samples compacted at 1.4 GPa (open circles) and 0.32 GPa (triangles) from commercial powder. The PAS data were taken at room temperature; no sintering aids were used. After [26].

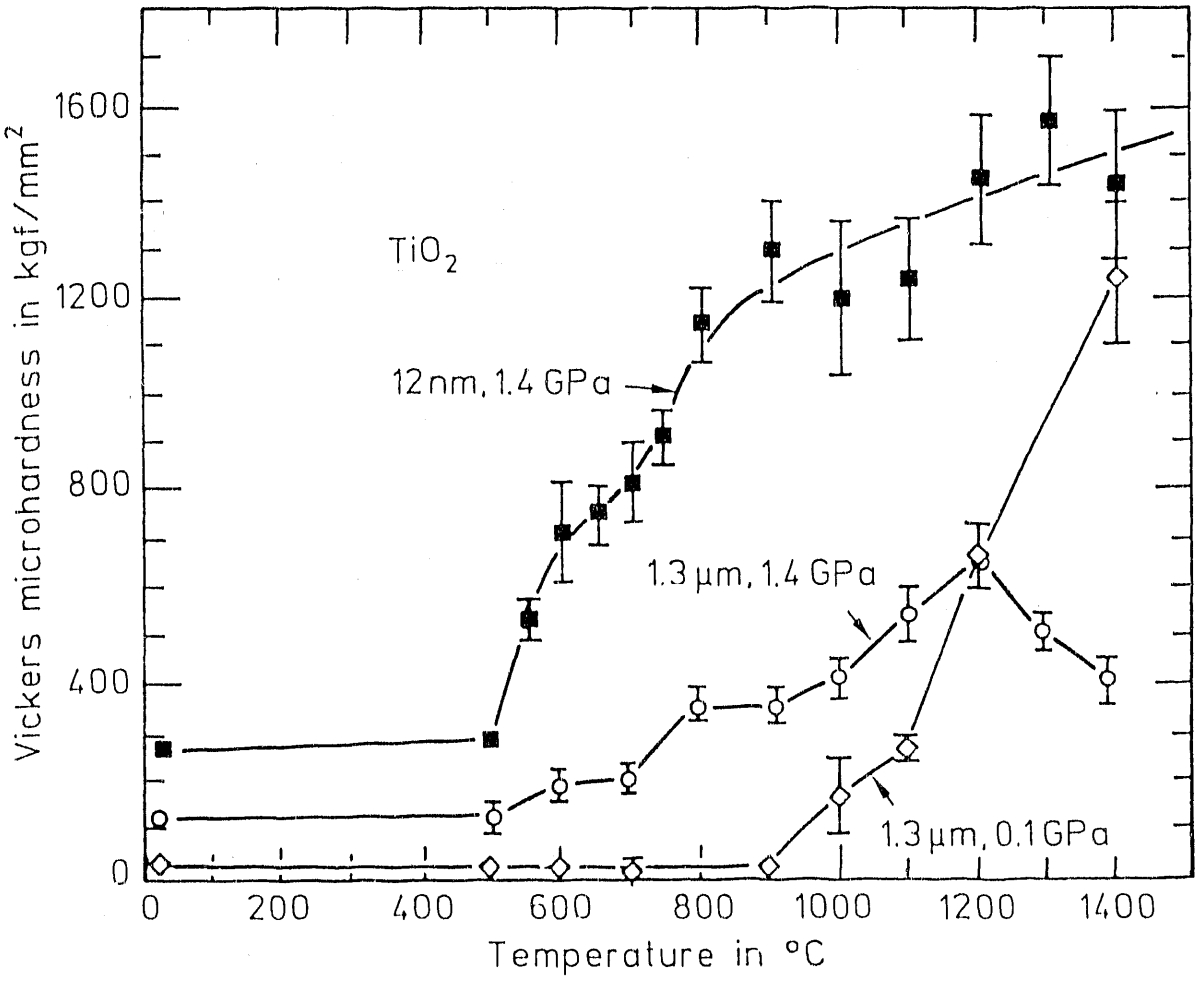

Figure 6. Vickers microhardness of TiO_2 (rutile) measured at room temperature as a function of one-half hour sintering at successively increased temperatures. Results for a nanophase sample (squares) with an initial average grain size of 12nm compacted at 1.4 GPa are compared with those for coarser-grained compacts with 1.3 µm initial average grain size sintered with the aid of polyvinyl alcohol from commercial powder compacted at 0.1 GPa (diamonds) and 1.4 GPa (crosses). From [26].

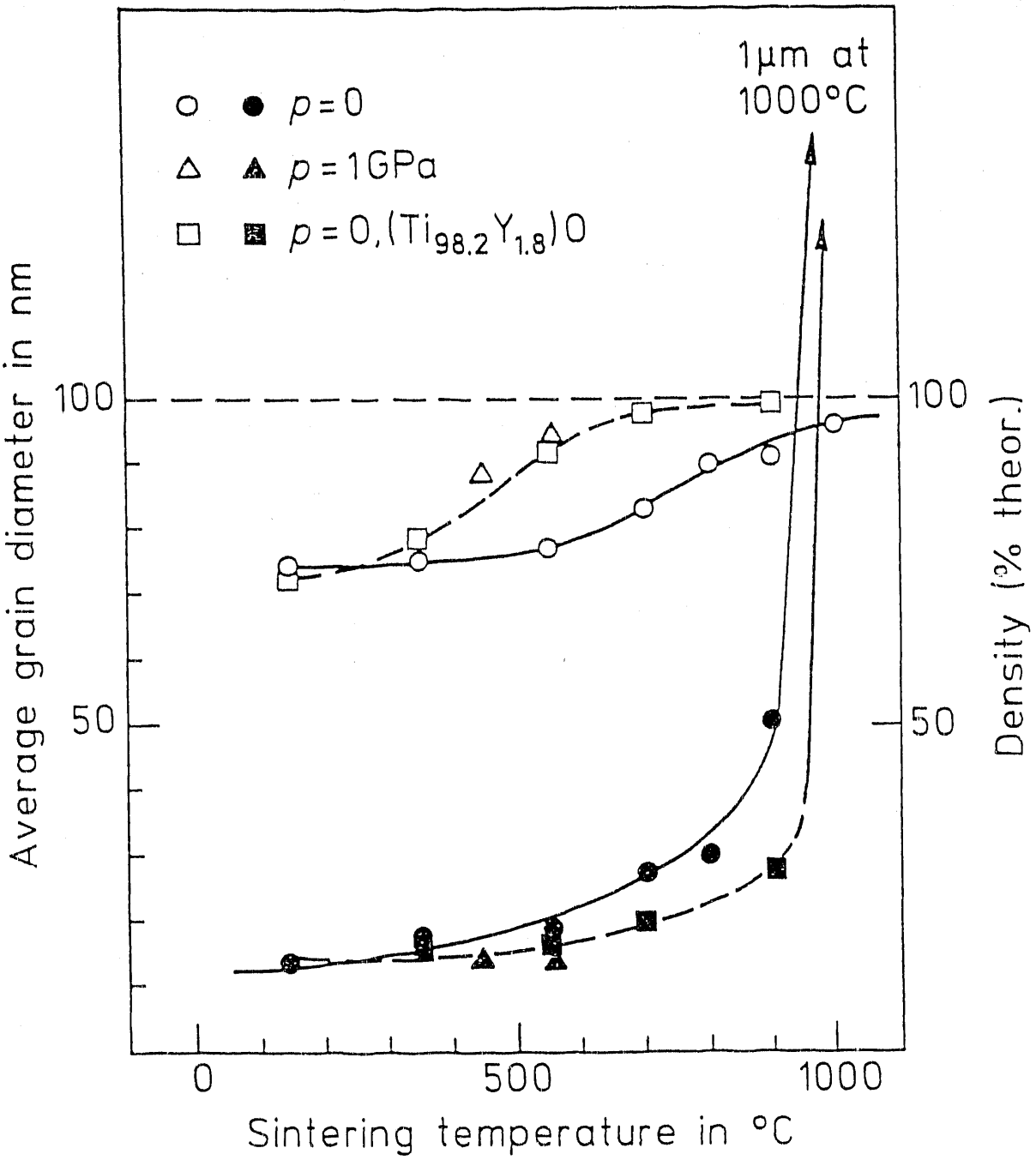

Figure 7. Density (open symbols) and grain size (closed symbols) of nanophase TiO_2 as a function of sintering temperature. Included are data for sintering at atmospheric pressure, pressure-assisted sintering, and Y-doped nanophase TiO_2. After [54].

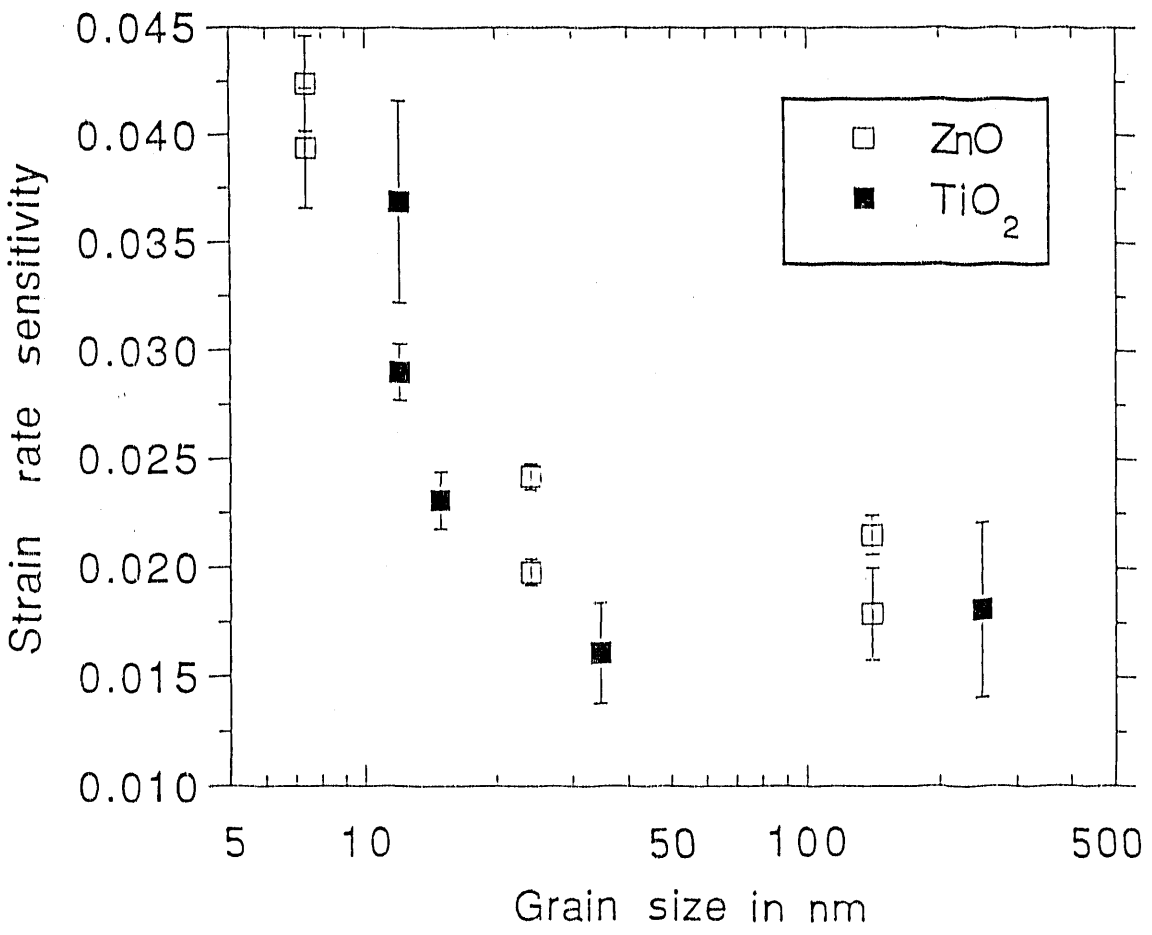

Figure 8. Strain rate sensitivity of nanophase TiO_2 [60] and ZnO [61] as a function of grain size. The strain rate sensitivity was measured by a nanoindentation method and the grain size was determined by dark-field transmission electron microscopy.

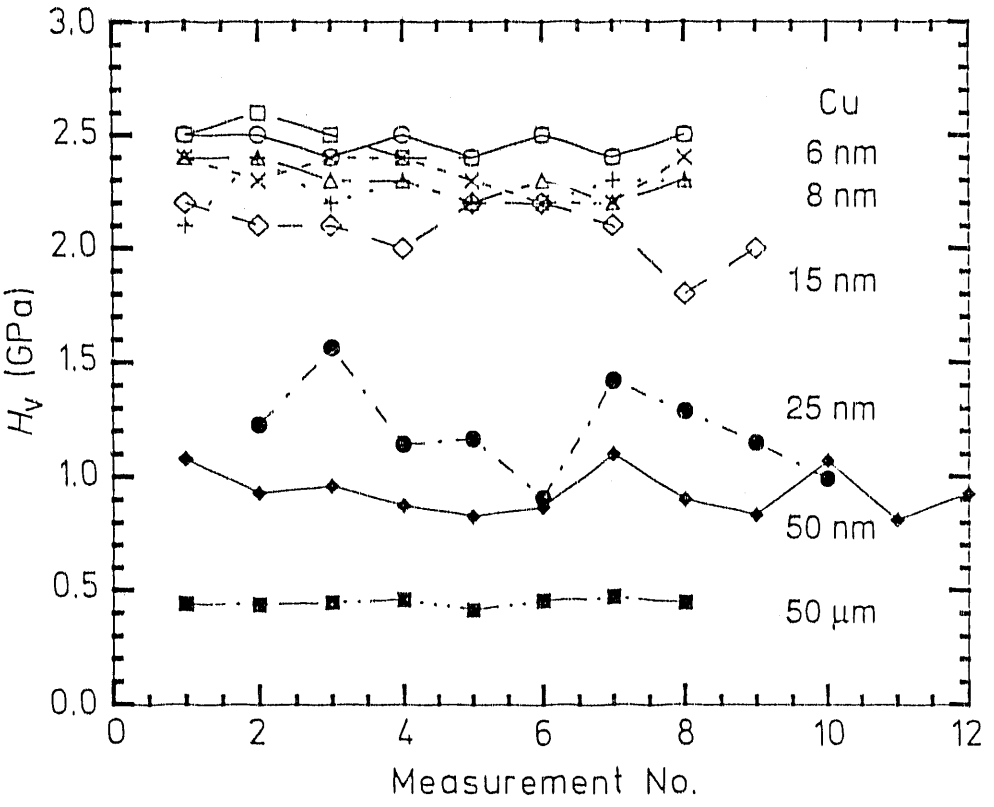

Figure 9. Vickers microhardness measurements at various positions across several nanophase Cu samples ranging in grain size from 6 to 50 nm, compared with similar measurements from an annealed conventional 50 μm grain size Cu sample. After [62].

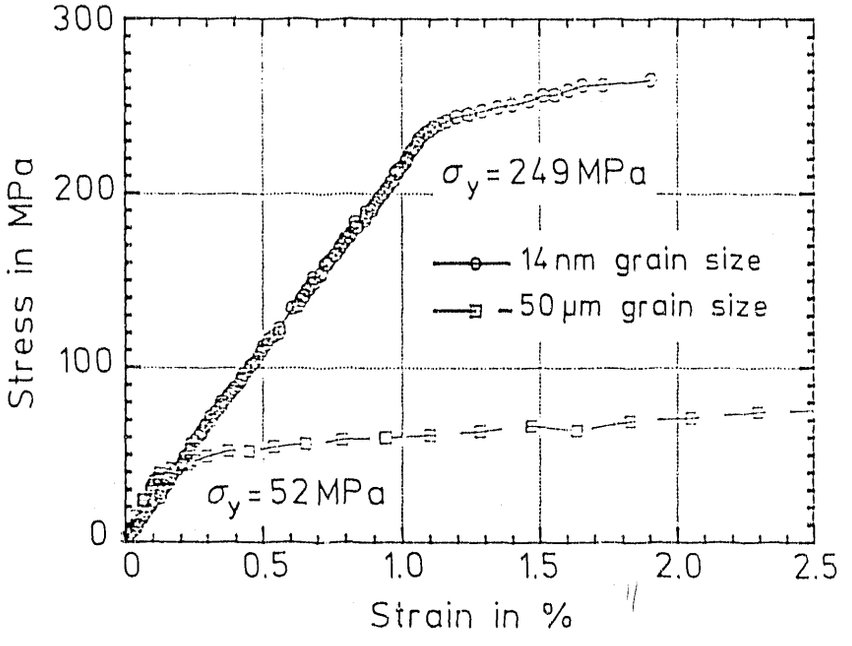

Figure 10. Stress-strain curve for a nanophase (14 nm) Pd sample compared with that for a coarse-grained (50 μm) Pd sample. The strain rate $d\varepsilon/dt \approx 2 \times 10^{-5}\ s^{-1}$. After [64].

END

DATE
FILMED
5/13/92